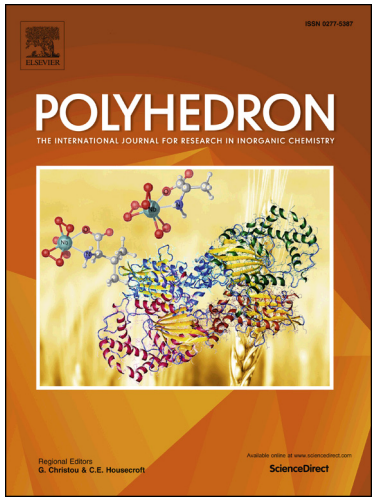

Synthesis, structure and magnetic properties of an unusual oligonuclear iron(III)-cobalt(III) compound with oxido-, sulfato- and cyanido-bridging ligands

Fatima Setifi, Zouaoui Setifi, Piotr Konieczny, Christopher Glidewell, Samia Benmansour, Carlos J. Gómez-García, Fernande Grandjean, Gary J. Long, Robert Pelka, Jan Reedijk

PII: S0277-5387(18)30657-0
DOI: https://doi.org/10.1016/j.poly.2018.10.021
Reference: POLY 13495

To appear in: *Polyhedron*

Received Date: 13 August 2018
Revised Date: 29 September 2018
Accepted Date: 5 October 2018

Please cite this article as: F. Setifi, Z. Setifi, P. Konieczny, C. Glidewell, S. Benmansour, C.J. Gómez-García, F. Grandjean, G.J. Long, R. Pelka, J. Reedijk, Synthesis, structure and magnetic properties of an unusual oligonuclear iron(III)-cobalt(III) compound with oxido-, sulfato- and cyanido-bridging ligands, *Polyhedron* (2018), doi: https://doi.org/10.1016/j.poly.2018.10.021

Manuscript for: ***Journal*** *Polyhedron. Revised October; ms number: POLYD-18-00778*

Synthesis, structure and magnetic properties of an unusual oligonuclear iron(III)-cobalt(III) compound with oxido-, sulfato- and cyanido-bridging ligands

Fatima Setifi[a,*], Zouaoui Setifi[a,b], Piotr Konieczny[c], Christopher Glidewell[d], Samia Benmansour[e], Carlos J. Gómez-García[e,*], Fernande Grandjean[f], Gary J. Long[f,*], Robert Pelka[c], Jan Reedijk[g,*]

[a] *Laboratoire de Chimie, Ingénierie Moléculaire et Nanostructures (LCIMN), Université Ferhat Abbas Sétif 1, Sétif 19000, Algeria*

[b] *Département de Technologie, Faculté de Technologie, Université 20 Août 1955-Skikda, Skikda 21000, Algeria*

[c] *Institute of Nuclear Physics, Polish Academy of Sciences, Radzikowskiego 152, 31-342 Krakow, Poland*

[d] *School of Chemistry, University of St Andrews, Fife KY16 9ST, United Kingdom*

[e] *Instituto de Ciencia Molecular (ICMol). Dpt. Química Inorgánica Catedrático José Beltrán, 2. 46980 Paterna Valencia, Spain.*

[f] *Department of Chemistry, Missouri University of Science and Technology, University of Missouri, Rolla, Missouri 65409-0010, USA*

[g] *Leiden Institute of Chemistry, Leiden University, P.O. Box 9502, 2300 RA Leiden, The Netherlands*

Abstract:

The synthesis, characterization, structure and magnetic properties of a hexametallic mixed-metal iron(III)-cobalt(III) compound are described. The compound has been characterized by standard spectroscopic and analytical methods to determine its composition. Single-crystal X-ray diffraction has shown that the asymmetric unit consists of discrete dinuclear dicationic units of {(μ-oxido-μ-[sulfato-*O1,O2*])bis[tris(2-pyridyl-methyl)amineiron(III)]}$^{2+}$, herein designated as Fe12, and two half-dinuclear dianionic units of {(μ-oxido)bis[<μ-cyanido-*κN*-pentacyanidocobaltato(III)><tris(2-pyridylmethyl)-amine>iron(III)]}$^{2-}$ units, herein designated as Fe33a and Fe44b, generating the overall composition $Co_2Fe_4O_2(CN)_{12}(tpa)_4$, **1**, where tpa is tris(2-pyridylmethyl)amine. X-ray structural results and thermogravimetric and differential scanning calorimetry measurements also indicate that the compound, depending upon its history may contain up to nine interstitial waters of hydration, herein designated as **1**$(H_2O)_9$.

In the dinuclear dicationic unit, the bridging Fe-O-Fe bond in Fe12 is bent and there is also an Fe-O-S-O-Fe sulfato-based bridge with an angle of 132.8º. In contrast, in the two dinuclear dianionic units, Fe33a and Fe44b, the Fe-O-Fe bond angle is crystallographically constrained to be linear. The Co-CN-Fe bonds are almost co-linear, with Co-C-N angles of 176º and C-NFe angles of 169º-. In each species the tpa ligand is tripodal tetradentate with the tertiary amine *trans* to the sulfato ligand or to the cyanide ligand in the dianions or the bridged oxido ligand in the dications. Bond lengths and angles are all in the typical range for Fe(III) and Co(III) compounds.

The magnetic behavior of **1**$(H_2O)_9$, obtained upon cooling from 300 to 2 K, reveals a strong antiferromagnetic interaction between the Fe(III) ions in each dinuclear unit. Attempts to discriminate between the two Fe(III) dinuclear units in **1**$(H_2O)_9$ have in all cases led to two very different Heisenberg isotropic exchange coupling constants, namely J = **-**220(2) and **-**716(32) cm^{-1} for **1**$(H_2O)_9$; i.e.. one of the dinuclear units, probably the Fe12 unit, is so strongly antiferromagnetically coupled that it is close to diamagnetic between 2 and ca. 250 K and has a Heisenberg *S* = 0 ground state.

Keywords: Iron(III); Cobalt(III); Cyanide; Oxido-bridges; Antiferromagnetism

*Corresponding authors.

E-mail addresses: fat_setifi@yahoo.fr (F. Setifi), carlos.gomez@uv.es (C. J. Gómez-García), glong@mst.edu (G.J. Long), reedijk@chem.leidenuniv.nl (J. Reedijk).

†Electronic supplementary information (ESI) available. CCDC 1812913 for **1**. For ESI and crystallographic data in CIF or other electronic format see DOI: #####

1. Introduction

Mixed-metal compounds with bridging ligands have been of interest for quite some time, [1-5] both because of their magnetic exchange interactions and because similar units occur in nature in a variety of proteins and enzymes [6]. Among these compounds iron(II) and iron(III) coordination compounds are prominent in having an oxide bridge, that may be either linear or bent [7-12]. The interest in such iron(II) and iron(III) compounds largely stems from magnetic exchange interactions between the metal ions [13-16] and many species having the Fe(III)-O-Fe(III) bridge structure are found in the Cambridge Crystallographic Database [17, 18].

In the last few decades interest has also arisen in homo- and heteronuclear species bridged by a cyanide ligand [19-24]. The versatility of cyanide ligands as bridges is based on their ability to often act as a rigid end-on ligand bridge and, due to the linear and rigid geometry of the CN groups, often rather co-linear M-CN-M species are found, although slight bending at the C-N-M angle may occur [19, 20].

In order to explore the combination of oxido and cyanido bridging, we have used a mixture of Fe(III) and Co(III) in combination with the common tripodal tetradentate ligand tris(2-pyridylmethyl)amine, abbreviated as tpa. Herein we report on the synthesis of a unique mixed-metal compound based on Co(III) and Fe(III). The characterization and structure determination of the compound has been performed by infrared spectroscopy, elemental analysis, thermogravimetric and differential scanning calorimetry, and single crystal X-ray crystallography. The magnetic properties were studied in detail upon cooling from 300 to 2 K in order to explore the dinuclear Fe(III) exchange interactions in **1**$(H_2O)_9$; the pseudo-octahedral Co(III) ions are diamagnetic.

2. Experimental Results

2.1. Reagents, starting materials and synthesis techniques with characterization.

The starting products used for the synthesis of **1**, i.e., $FeSO_4 \cdot 7H_2O$, tris(2-pyridyl-methyl)amine and $K_3[Co(CN)_6]$ were purchased from Sigma–Aldrich and used without further purification.

The synthesis recipe followed was: A mixture of a methanol solution (2 mL) of tpa (0.1 mmol, 29 mg) and an aqueous solution (2 mL) of $FeSO_4 \cdot 7H_2O$ (0.1 mmol, 28 mg) was layered onto an aqueous solution (3 mL) of $K_3[Co(CN)_6]$ (0.1 mmol, 33 mg) in a test tube. The tube was sealed and left undisturbed at room temperature. Slow diffusion of the resulting solution afforded red crystals of **1** within two weeks, which were filtered and carefully air-dried between filter paper. No further drying was applied.

Analyses for undried samples used for powder X-ray diffraction, thermogravimetric, and magnetic measurements agree with $C_{84}H_{90}N_{28}O_{15}SCo_2Fe_4$, abbreviated as **1**$(H_2O)_9$, with a molecular mass of 2105.13 g/mol and calc. values C, 47.93 %, H, 4.31 % and N, 18.63 %. The observed values are C, 48.08 %, H, 4.15 % and N, 18.22 %.

Apparently during the preparation air oxidation of Fe(II) to Fe(III) has occurred in the presence of the tpa ligand. Main non-ligand IR data (ν/cm^{-1}): ν(C≡N): 2124(vs); $\nu(SO_4)$: 1138(s), 1098(m), 995(m), 601(w). Broad bands ascribed to lattice water are at 3265 and 3393 cm^{-1}. Strong ligand bands are observed at 855, 869, 893, 919, 944, 1110, 1439, 1487, 1574, 3072 cm^{-1}.

Elemental analyses (C, H and N) were performed using a Perkin-Elmer 2400 series II CHN analyser. Infrared spectra were recorded in the range 4000–400 cm^{-1} as KBr pellets on a FT-IR EXCALIBUR FTS-3000 spectrometer.

2.2. X-ray crystallography

Diffraction data were collected at 293 K using a Bruker APEXII CCD diffractometer and graphite- monochromatised Mo-Kα (λ = 0.71073 Å) radiation. Data collection, cell refinement and data reduction were performed using APEX2 and absorption correction with SADABS [25]. Details of the crystal data, data collection and structure refinement are summarized in Table 1. The structure was solved by direct methods using SHELXS-97 [26] and refined by full-matrix least squares on F^2 with all data, using SHELXL-2014 [26]. All H atoms bonded to C atoms were located in difference maps, and then treated as riding atoms in geometrically idealised positions with C-H distances of 0.93 Å (pyridyl) or 0.97 Å (CH_2) and with $U_{iso}(H) = 1.2\ U_{eq}(C)$. Fourteen low-angle reflections, which had all been attenuated by the beam stop, were omitted from the data set. Conventional refinement of the ionic components converged only to $R_1 = 0.0975$ and $wR_2 = 0.3202$, and the difference map at this point contained a substantial number of significant but isolated maxima. Accordingly, two parallel refinements were then undertaken. In one, the difference peaks

which were within a plausible hydrogen-bonding distance either of potential donors or acceptors in the ionic components or of each other, were all assigned as the O atoms of partial-occupancy water molecules: for all of these sites, the atomic coordinates and the site occupancies were independently refined with U_{iso}(O) fixed at 0.07 Å^2 in each case. However, it did not prove possible to identify any H atom sites associated with these putative O atoms, but this refinement converged to R_1 = 0.0559 and wR_2 = 0.1861 for 1175 refined parameters.

The $C_{84}H_{90}N_{28}O_{15}SCo_2Fe_4$ stoichiometry corresponds to an asymmetric unit of **1**$(H_2O)_9$ consisting of one dication, Fe12, and two half-dianions, Fe33a and Fe44b, with their respective central oxygen situated on an inversion centre. In a second refinement, the structure from the initial refinement was subjected to the SQUEEZE procedure [27] within PLATON [28] and the subsequent refinement then converged to R_1 = 0.0431 and wR_2 = 0.1038, for rather fewer refined parameters than before, 1129, and with somewhat better precision for the geometric parameters as compared with the hydrated refinement model. After the final refinement, there were four bad outlier reflections, all of which were rather weak with values of Fc/Fc(max) in the range 0.009 - 0.044: in the absence of any convincing reason for their omission, they were retained in the data set. The SQUEEZE results indicated a total of ca. 176 electrons per unit cell associated with the partial occupancy water molecules, corresponding to a sum total of ca. 18 water molecules per unit cell, or 9 molecules per mole of **1**, in fair agreement with the elemental and thermogravimetric analysis, see the electronic supplementary information. Therefore, the results of this latter refinement are reported herein and below are referred to as **1**$(H_2O)_9$. The water molecules, shown from elemental analysis, however, could not be located and refined. Hence, it was decided to present the structural details of this latter refinement after squeeze, ignoring the water molecules present in the voids. The details for the structure and refinement are listed in Table 1.

Table 1. Crystal data and structure refinement parameters for compound **1**

	Compound **1**
Empirical formula	$C_{84}H_{90}N_{28}O_{15}SCo_2Fe_4$
Formula weight (g/mol)	1943.01
Temperature (K)	293(2)
Wavelength (Å)	0.71073
Crystal system	triclinic
Space group	*P-1*
Unit cell dimensions	
a (Å)	11.501(5)
b (Å)	20.767(8)
c (Å)	21.460(8)
α (°)	91.530(2)

β (°)	99.688(8)
γ (°)	105.268(9)
Volume (Å^3)	4860.6(3)
Z	2
Density (calculated) (g/cm^3)	1.328
Absorption coefficient (mm^{-1})	0.999
F(000)	1988
Index ranges	$-15 \le h \le 15$
	$-27 \le k \le 27$
	$-28 \le l \le 28$
Reflections collected	111631
Independent reflections	24749 [$R_{(int)}$ = 0.056]
Refinement method	Full-matrix least-squares on F^2
Data/restraints/parameters	24749/0/1129
Goodness-of-fit on F^2	1.022
Final R indices [$I>2\sigma(I)$]	R_1 = 0.0431
	wR_2 = 0.1038
R indices (all data)	R_1 = 0.0774
	wR_2 = 0.1181
Largest diff. peak and hole(e.Å^{-3})	+0.500 and –0.384

2.3. Magnetic measurements

Magnetic susceptibility measurements of a polycrystalline sample of **1**$(H_2O)_9$ have been carried out upon cooling from 300 to 2 K in an applied field of 500 Oe with a Quantum Design MPMSXL7 SQUID magnetometer. Because this sample was not dried before the magnetic measurements, it contained water that cannot be ignored in the analysis of the magnetic properties. The best estimate of the number of water molecules per mole of **1** is nine as indicated by the above analysis of the single crystal X-ray diffraction refinement and the thermogravimetric analysis (see supporting information). Hence, the composition of the sample used for the magnetic measurements is referred to as **1**$(H_2O)_9$ with a molecular mass of 2105.13 g/mol. The discussion of the magnetic measurements below is for **1**$(H_2O)_9$ and some results in terms of **1** are shown in the electronic supplementary information and provide a range of fitted parameters for the in principle uncertain number of crystallization water molecules.

All reported fits of the temperature dependence of the magnetic susceptibility, χ_M, were carried out with the gnuplot code [29], which uses an implementation of the nonlinear least-squares Marquardt-Levenberg algorithm. The goodness of fit is calculated as the root mean-square, rms, of the deviation between calculated and measured values.

All molar magnetic susceptibilities have been corrected for a core diamagnetic contribution by subtracting –0.001090 cm^3/mol from the observed molar susceptibility of **1**$(H_2O)_9$; the Pascal constants were obtained from Bain and Berry[30].

Subsequent to the above magnetic susceptibility measurements, the results have been duplicated within experimental uncertainties on a second newly prepared sample, isothermal magnetization measurements were performed at 2 K over an applied field range of ±7 T.

Details on the thermogravimetric analysis and X-ray powder diffraction pattern of the sample used for magnetic measurements are given in the supplementary information.

3. Results and discussion

3.1. Synthesis and characterization

The isolation and characterization of $Co_2Fe_4O_2(CN)_{12}(tpa)_4$, **1**, was primarily performed by using elemental analysis and IR spectroscopy. Repeated syntheses using various temperatures of 10 to 40 °C and various times indicated that the synthesis was reproducible and samples analysed best for **1**$(H_2O)_9$.

3.2. Description of the crystal structure

Compound **1** is ionic and contains one dinuclear dication of composition $[\{(tpa)Fe\}_2(SO_4)O]^{2+}$ [tpa = tris(2-pyridylmethyl)amine], in which the bridging oxygen O1 lies on a general position, (see Fig. 1a for the dication Fe12 bridged by O1) and two independent anions of composition $[\{(tpa)Fe(Co(CN)_6)\}_2O]^{2-}$, in which the bridging oxygens O3 and O4 occupy a centre of inversion (see Fig. 1b for the dianion Fe33a bridged by O3) and see Fig. S1 for the very similar Fe44b dianion bridged by O4.

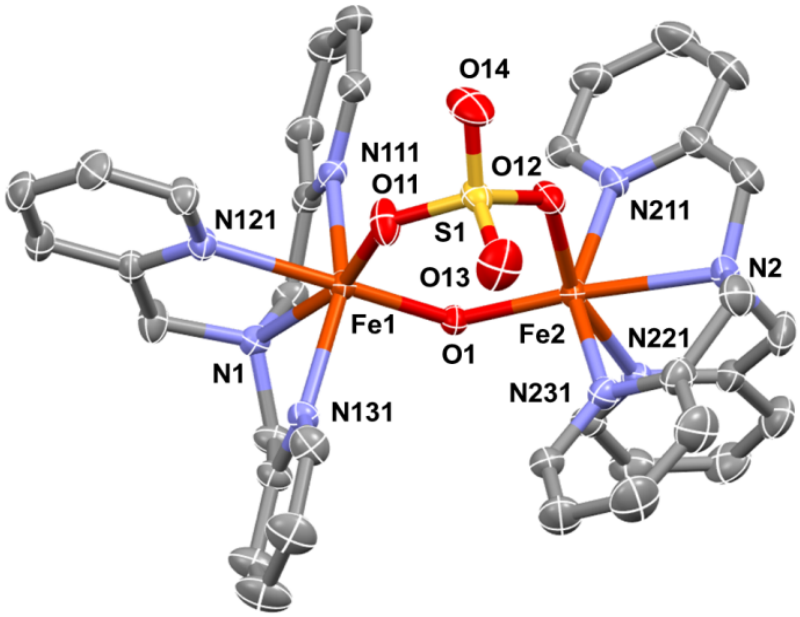

a) ***The dicationic unit Fe12***

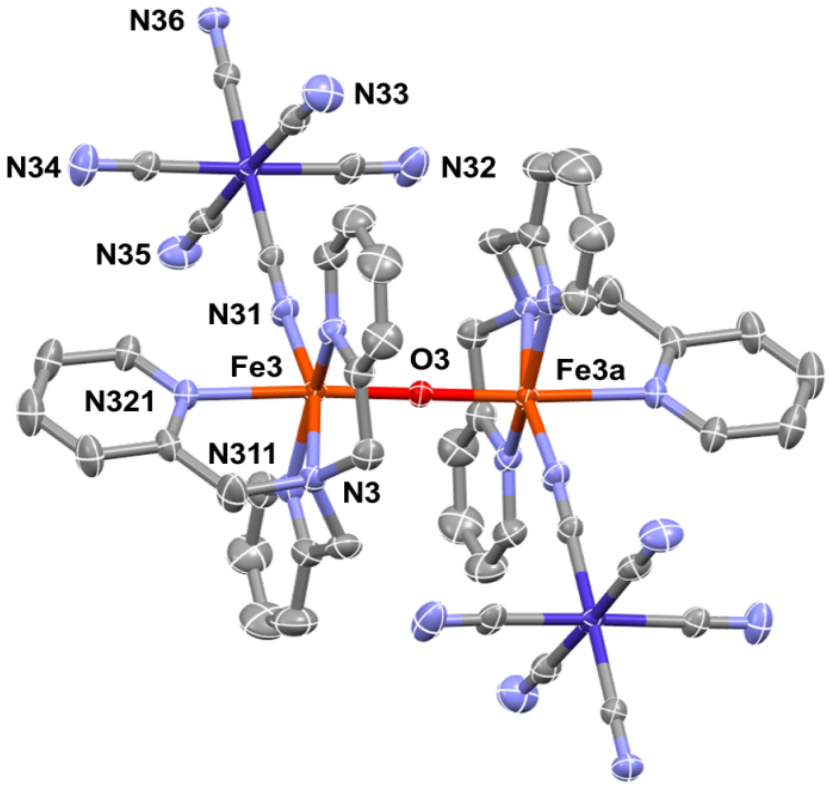

b) The dianionic unit Fe33a

Figure 1. The independent diionic components of compound **1** *with displacement ellipsoids drawn at the 30 % probability level for (a) the dinuclear Fe12 dication and (b) the dinuclear Fe33a dianion. The structure of the dinuclear Fe44b dianion is very similar to that shown for Fe33a and is shown in Fig. S1. For clarity the H and C labels have been omitted. The centre of the Fe33a and Fe44b dianions at the bridging oxygen are at symmetry positions (–x,1–y,–z) and (–x,1–y,1–z), respectively.*

It should be noted that the asymmetric unit for **1** contains one Fe12 dication and one-half each of the Fe33a and Fe44b dianions to yield a total of four Fe(III) ions in **1**. The triclinic unit cell with Z = 2 thus contains two Fe12 dications, one Fe33a and one Fe44b dianions, yielding an overall composition $[\{(tpa)Fe\}_2(SO_4)O]$ $[\{(tpa)Fe(Co(CN)_6)\}_2O]$ for **1** (see Fig. 2).

In the dication, the two (tpa)Fe units are bridged by an oxido ligand and by a sulfato(*O,O'*) ligand to yield an Fe1···Fe2, Fe(III) to Fe(III) distance of 3.302(2) Å. In each (tpa)Fe unit of the dication, the three pyridyl N atoms adopt an equatorial configuration with Nx11 and Nx31 (x = 1 or 2) in mutually *trans* sites. However, at Fe1, the third pyridyl N (N121) is *trans* to the oxido ligand, whereas at Fe2, it is the central N2 of the tpa unit which is *trans* to the bridging oxido ligand, an arrangement that thereby precludes any internal symmetry in the dication.

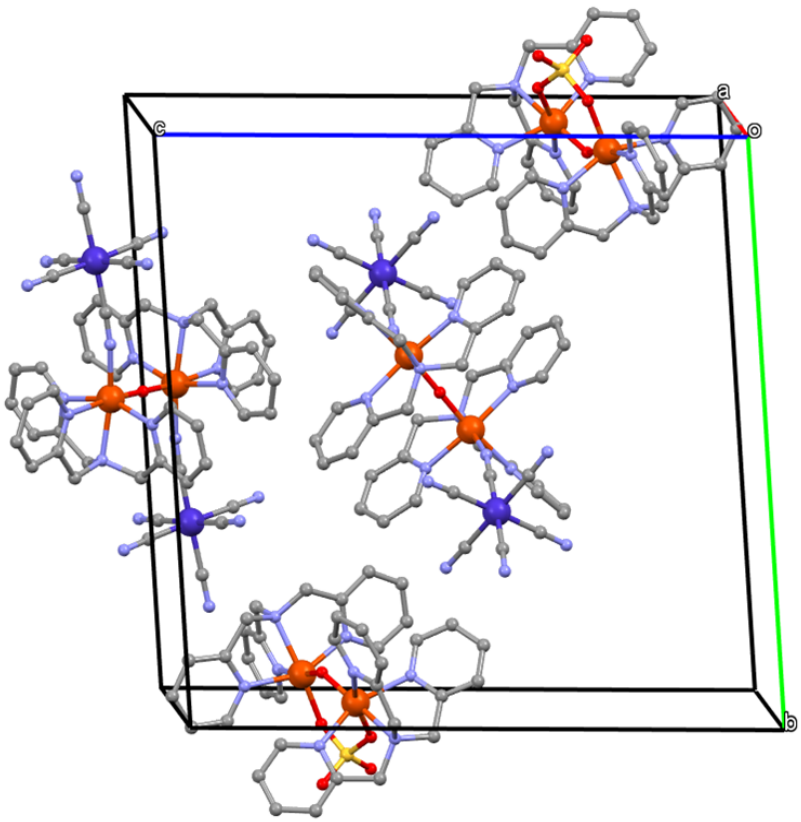

Figure 2. The unit-cell content showing two dinuclear Fe12 inversion-related bent dications on a general position, (x,y,z), and the dinuclear dianions, Fe33a and Fe44b, centred at (0,½,0) and (0,½,½), which are the positions of the O3 and O4 bridging oxygens, respectively.

Each of the two independent dianions lies across a centre of inversion such that in each dianion, not only are the two Fe(III) centres equivalent, but the Fe-O-Fe bridge is strictly linear, with Fe···Fe Fe(III) to Fe(III) distances of 3.581(2) and 3.588(2) Å, in the Fe33a and Fe44b units, respectively. It should be noted that in each of the dianions Fe33a and Fe44b the Fe(III) to Fe(III) distances are ca. 8 % longer than the distance of 3.302(2) Å observed in the dication Fe12. In each of the Fe33a and Fe44b dianions the pyridyl N atoms of the tpa component again adopt an equatorial configuration with Nx11 and Nx31 (x = 3 or 4) *trans* to one another and with Nx21 *trans* to the bridging oxido ligand. Thus in each dianion, the central N of the tpa is *trans* to one of the N atoms from the $[Co(CN)_6]^{3-}$ unit acting as the sixth ligand to the Fe(III). The shortest Co···Fe distances in the two dianions are Co3···Fe3 at 5.030(2) Å and Co4···Fe4 at 5.022(2) Å. Relevant bond distances are given in Table 2, whereas bond angles are presented in Table S1. Refinement after SQUEEZE gave essentially the same results within experimental error, and are not tabulated again.

Table 2 Relevant bond lengths (Å) around the Fe(III) and Co(III) ions for **1**

Fe1 O1	1.8123(17)	O4 Fe4	1.7942(6)	Co4 C41	1.879(3)
Fe1 O11	1.941(2)	Fe4 N41	2.041(2)	Co4 C42	1.894(3)
Fe1 N131	2.138(2)	Fe4	2.140(2)	Co4 C46	1.901(3)

		N411			
Fe1 N111	2.151(2)	Fe4	2.140(2)	Co4 C45	1.902(3)
		N431			
Fe1 N121	2.191(2)	Fe4 N4	2.183(2)	Co4 C43	1.906(3)
Fe1 N1	2.193(2)	Fe4	2.201(2)	Co4 C44	1.913(3)
		N421			
Fe2 O1	1.7922(17)	Co3 C31	1.876(3)	C41 N41	1.154(3)
Fe2 O12	2.0057(19)	Co3 C32	1.895(3)	C42 N42	1.143(3)
Fe2 N231	2.130(2)	Co3 C36	1.902(3)	C43 N43	1.138(4)
Fe2 N221	2.131(2)	Co3 C35	1.903(3)	C44 N44	1.152 (4)
Fe2 N211	2.155(2)	Co3 C33	1.907(3)	C45 N45	1.148(4)
Fe2 N2	2.243(2)	Co3 C34	1.908(3)	C46 N46	1.141(3)
O3 Fe3	1.7903(6)	C31 N31	1.152(3)		
Fe3 N31	2.035(2)	C32 N32	1.142(4)		
Fe3 N311	2.133(2)	C33 N33	1.142(4)		
Fe3 N331	2.137(2)	C34 N34	1.146(4)		
Fe3 N3	2.183(2)	C35 N35	1.145(4)		
Fe3 N321	2.231(2)	C36 N36	1.149(3)		

The structure contains just one significant hydrogen bond between the ions, linking the dianions of type Fe44b into a ribbon containing edge-fused $R^2_2(22)$ rings aligned parallel to the [100] direction (see Fig. 3); the donor is provided by one of the CH_2 groups and the acceptor by one of the cyanide groups in $[Co(CN)_6]^{3-}$ (see the dashed lines).

The relative orientation of the three different units and their codes are presented in Figure 4, that also indicates the magnetic exchange parameters used (*vide infra*).

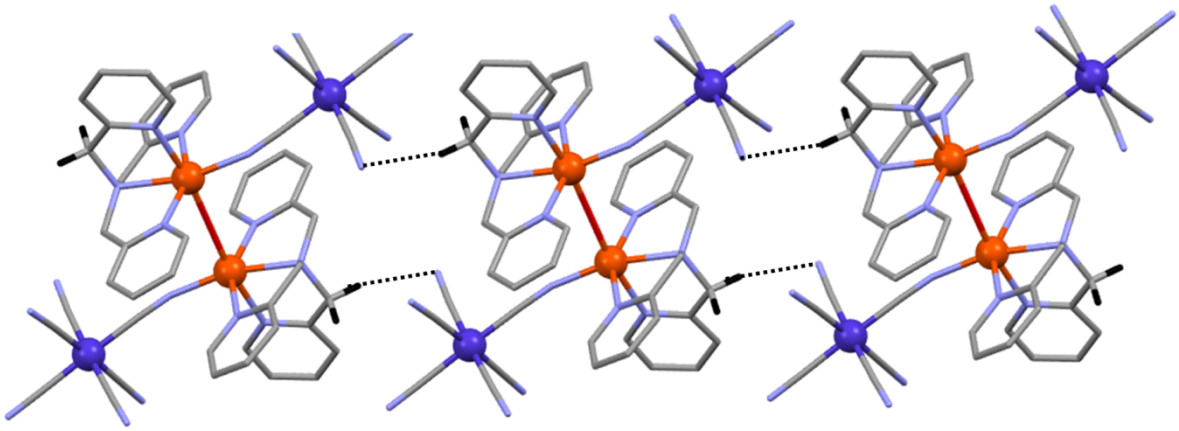

Figure 3: Packing showing weak hydrogen bonding between a CN group and a CH_2 of the Fe44 unit.

The discussion of the structural details of **1** in comparison with the literature, will be presented in more detail below in section 3.3, together with the magnetic analysis.

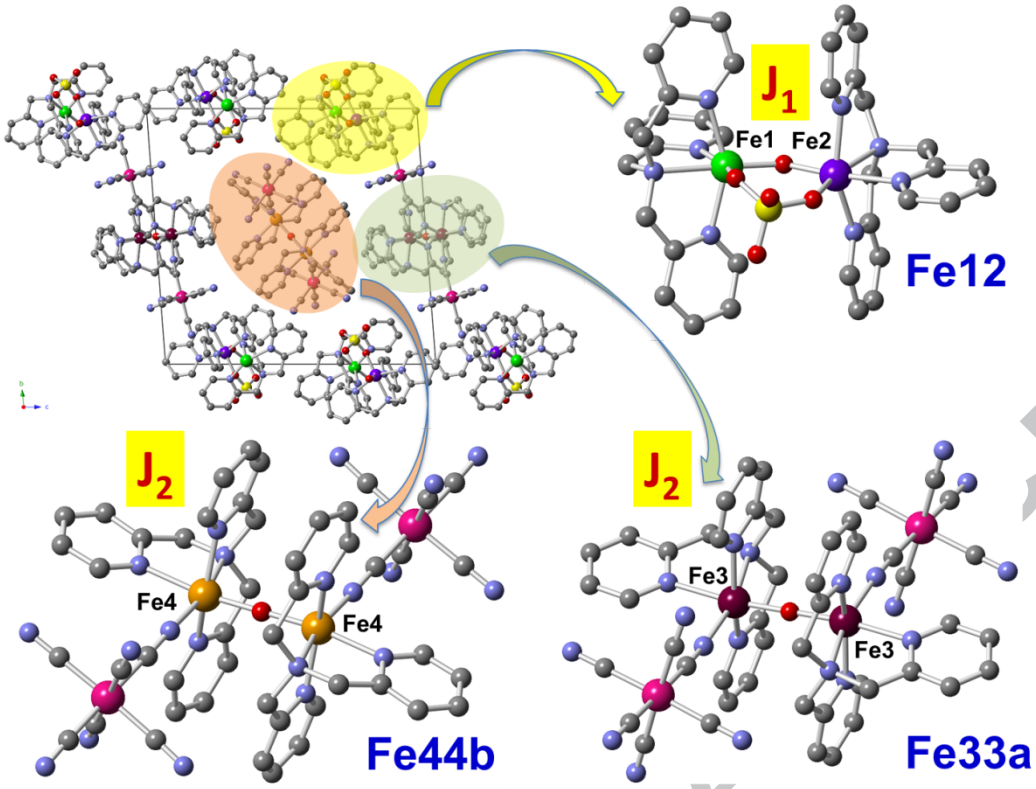

*Figure 4. Relative orientation, unit coding and the Heisenberg isotropic exchange parameters used for compound **1**.*

3.3. **Magnetic properties**

An analysis of the magnetic properties of **1**$(H_2O)_9$ presents a challenge, because its molar magnetic susceptibility, χ_M, see Figure 5, or for **1**, see Figure S2, is very small, as might be expected of a compound whose asymmetric unit consists of a dinuclear Fe(III)···Fe(III) dication, Fe12, with both an oxido- and a sulfato-bridged structure, and two very similar half-dinuclear Fe(III)-O-Fe(III) dianions, Fe33a and Fe44b. Extensive antiferromagnetic exchange coupling is expected in both the dication and the dianions. The contributions to the magnetic susceptibility of the Fe12 dication and of the two half-dianions have the same weight, as is shown in functions (1) and (3), below. Further, the analysis must include both the second-order Zeeman contribution, $N\alpha$, to χ_M, and the presence of a trace of always present paramagnetic high-spin Fe(III) impurity.

The presence of strong antiferromagnetic properties in **1**$(H_2O)_9$ is further confirmed in Figure 5, which indicates that the product, $\chi_M T$, per formula unit of **1**$(H_2O)_9$, i.e. the $\chi_M T$ per mole of four Fe(III) ions, exhibits a 300 K value of 1.451(2) cm^3 K/mol, a value that is well below the expected 17.50 cm^3 K/mol value for four magnetically independent S = 5/2 high-spin Fe(III) ions with g = 2. On cooling the $\chi_M T$ of **1**$(H_2O)_9$ exhibits a continuous almost linear decrease and reaches a value of 0.123(2) cm^3 K/mol at 50 K.

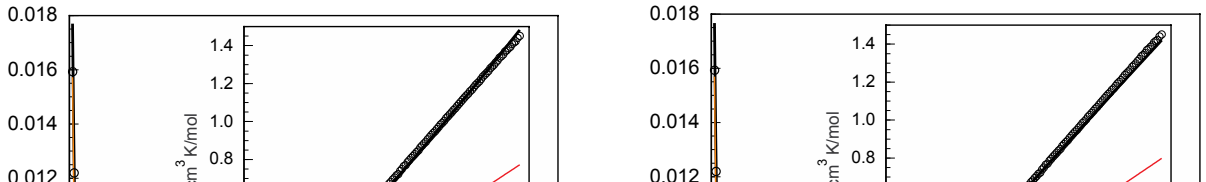

*Figure 5. The temperature dependence, measured upon cooling from 300 to 2 K in a 500 Oe applied field, of χ_M for **1**$(H_2O)_9$ and the corresponding $\chi_M T$ values in the inset, open points, and their fits with functions (1), left, and (2), right. The components of the fit are J_2 or J in red, J_1 in blue, $N\alpha$ in purple, and a high-spin Fe(III) impurity in orange; the sum of these components leads to the black line through the data points, a line that is mostly obscured by the data points; the J_1 blue component is also mostly obscured in the left figure.*

The observed temperature dependence of χ_M suggests the presence of a strong antiferromagnetic Fe(III)-Fe(III) exchange coupling interaction in **1**$(H_2O)_9$. Indeed, the thermal variation of χ_M exhibits an almost constant χ_M between 300 and ~250 K followed by a gradual decrease on further cooling to a rounded minimum of 0.00244(3) cm^3/mol at 53.8 K. Upon further cooling of **1**$(H_2O)_9$ below 53.8 K χ_M exhibits a large increase to 0.0159(2) cm^3/mol at 2 K, a clear indication of the presence of a trace of a monomeric paramagnetic Fe(III) impurity, as is often observed in strongly antiferromagnetically exchange coupled iron(III) compounds.

Because **1**$(H_2O)_9$ exhibits strong antiferromagnetic exchange, we have fit the molar magnetic susceptibility, χ_M, measured upon cooling with the Heisenberg isotropic exchange coupling Hamiltonian, $\boldsymbol{H} = -J\boldsymbol{S}_1\cdot\boldsymbol{S}_2$, which has been discussed in detail by Kahn.[31] This analysis has been carried out for both compositions, **1**$(H_2O)_9$, see Figure 5 and **1**, see Figure S2.

As a consequence, the temperature dependence of χ_M measured at 500 Oe upon cooling from 300 to 2 K of **1**$(H_2O)_9$ and **1** has been fitted with function (1),

$$\chi_M(T) = \chi_{M,1}(T,g,J_1) + \chi_{M,2}(T,g,J_2) + N\alpha + yC_{Fe(III)}/T, \quad (1)$$

where J_1 corresponds to the antiferromagnetic exchange, in the dinuclear Fe12 dication, J_2 corresponds to the antiferromagnetic exchange, which is considered to be equivalent, in both of the half-dinuclear Fe33a and Fe44b dianions, g is the Landé-factor constrained to 2.00 as expected for high-spin Fe(III), $N\alpha$ is the second-order Zeeman contribution to χ_M resulting from the two Co(III) ions and perhaps to a lesser extent from the four Fe(III) ions present, $C_{Fe(III)}$ is the Curie constant in cm^3 K/mol for isolated impurity high-spin Fe(III) ions with S = 5/2 and g = 2, and y is the fractional amount of this impurity.

In a first fit, J_1 and J_2 were constrained to be equal in function (1). The resulting fit as shown in Figure S3 is rather poor. Second, J_1 and J_2 were independently refined and the resulting fit, shown in Figure 5 left with the resulting parameters given in Table 3, is excellent. Because, rather unexpectedly, J_1 is very negative, the contribution of the unit Fe12 to the magnetic susceptibility is essentially zero at all temperatures, i.e., the dinuclear unit behaves diamagnetically and effectively has a Heisenberg S = 0 electronic spin ground state. A fit with function (2),

$$\chi_M(T) = \chi_M(T,g,J) + N\alpha + yC_{Fe(III)}/T, \quad (2)$$

where J is the exchange coupling constant for units Fe33a and Fe44b, was carried out. The resulting fit is shown in Figure 5 right and even though its visual quality is as good as that shown on the left, its statistical quality is slightly, perhaps significantly, poorer.

Functions (1) and (2) correspond to the case in which the Fe(III) impurity is intrinsic to the sample preparation and function (3),

$$\chi_M(T) = (1 - y/4)\{\chi_{M,1}(T, g, J_1) + \chi_{M,2}(T, g, J_2)\} + N\alpha + yC_{Fe(III)}/T, \quad (3)$$

corresponds to the case in which the Fe(III) impurity is derived from the decomposition of a dinuclear Fe(III) species. Because the fits with function (3) yield statistically the same fits as those with functions (1) and (2), only the fit with function (1), which is the best fit, is discussed in detail below.

The best χ_M fit parameters for both compositions **1** and **1**$(H_2O)_9$, corresponding to the fit with functions (1) and (2) shown in Figures 5 and S2, are given in Table 3, a table which also gives the comparable fits obtained with function (3). The difference in the best parameters obtained for **1** and **1**$(H_2O)_9$ provides an uncertainty that is more realistic than the statistical uncertainties. It is important to note that there is often significant correlation between the fit parameters and the correlation coefficient matrix for each of the fits given in Table 3 are presented in the ESI in Table S2; in all cases the most significant and always negative correlation is found between J_2 and $N\alpha$.

Table 3. The best χ_M fit parameters obtained for **1** and **1**$(H_2O)_9$, with functions (1), (2) and (3) with $S_1 = S_2 = 5/2$ and $g = 2$. The statistical uncertainties are given in parentheses.

Compound	Function	J *or* J_2, cm^{-1}	J_1, cm^{-1}	$N\alpha$, cm^3/mol	y, %
1	1	–228(2)	–900(35)	0.00179(3)	0.630(5)
	2	–226(2)	-	0.00179(3)	0.629(5)
	3	–228(2)	–894(66)	0.00179(3)	0.630(5)
1$(H_2O)_9$	1	–220(2)	–716(32)	0.00197(3)	0.683(6)
	2	–214(2)	-	0.00198(3)	0.681(6)
	3	–220(2)	–712(32)	0.00197(3)	0.683(6)

In the fitting model we have included a contribution of one for Fe12 and one half for each Fe33a and Fe44b, because there are twice as many Fe12 species as Fe33a and Fe44b in the unit cell of **1** and likewise in **1**$(H_2O)_9$, see Figure 4, for their relative orientations. This model reproduces very well the magnetic properties of **1** or **1**$(H_2O)_9$, over the entire 2 to 300 K temperature range with g constrained to 2.0 and four variables, J_1, J_2, y, for a $S = 5/2$ paramagnetic impurity, and a temperature independent paramagnetic molar susceptibility, i.e., $N\alpha$, the second-order Zeeman contribution to χ_M, that is typical of the pseudo-octahedral Co(III) ions present in **1**. Indeed, the observed values of 0.00179(3) cm^3/mol for **1,** or 0.00197(3) cm^3/mol for **1**$(H_2O)_9$, are close to the value of 0.00162 cm^3/mol for two Co(III) ions in $SrTi_{0.65}Co_{0.35}O_3$ as reported by Pascanut et al.[32]

In the following, we present a very tentative assignment of the two different coupling constants to the Fe33a and Fe44b dinuclear species and the Fe12 species in **1**.

The fitted J_2 value of –220(2) cm^{-1} for **1**$(H_2O)_9$ is very typical of the exchange coupling constant found for several linear oxido-bridged Fe(III) compounds and, thus, this

value is assigned as the average exchange constant for the Fe33a and Fe44b dinuclear units; the Fe-O and Fe···Fe bond distances and angles for Fe33a and Fe44b are also consistent with this assignment, see Table 3. In contrast, the most unexpected aspect of the fits shown in Figure 5 and Figure S2 and the resulting values given in Table 3 is the very large negative J_1 value of –900(35) cm^{-1} found for **1** and likewise –716(32) cm^{-1} found for **1**$(H_2O)_9$, values which by default must be assigned to Fe12 which has both a bent Fe-O-Fe and a bent Fe-O-S-O-Fe bridging exchange pathway. However, it may be instructive to note that the Fe···Fe non-bonded distance for the Fe12 site is 3.302(2) Å, a value which is substantially shorter than the 3.581(2) and 3.588(2) Å Fe···Fe non-bonded distances found in Fe33a and Fe44b, respectively. Perhaps the shorter through-space distance in Fe12 promotes the observed enhancement of the antiferromagnetic exchange in this dinuclear unit.

Unfortunately, the magnetic results reported herein always yield the sum of the magnetic properties of all the Fe(III) ions present. In order to provide fundamental support for an assignment of the two exchange coupling constants to the sites in **1**, a future density functional theory study of the magnetic exchange pathways may be useful or required.

To obtain further insight in the magnetic properties, the magnetisation of **1** or **1**$(H_2O)_9$ has also been measured at 2 and 300 K in an applied field between ±7 T. The observed moments at 300 K are so small that the results were found unreliable. In contrast, at 2 K and at fields of ±6 T the observed moments are, in part, sufficient enough to yield reliable results, see Figure 6 (and Figure S4 for **1**). At 2 K the magnetisation is dominated by the high-spin Fe(III) impurity and thus the magnetisation, M, in units of Nβ has been simulated with the expression

$$M = aH + y(\mathrm{B}(H,g,S,T)), \quad (4)$$

where H is the applied field in Tesla and B is the Brillouin function calculated for g = 2, S = 5/2, and T = 2 K; the fitted a and y values are -4.854×10^{-3} and -5.259×10^{-3} Nβ/T and 0.63 and 0.68 %, for **1** and **1**$(H_2O)_9$, respectively. The first term represents the linear diamagnetic contribution to the magnetisation, whose slope of -4.854×10^{-3} or -5.259×10^{-3} Nβ/T has been obtained from a linear fit of the observed magnetisation between 2 and 6 T. In the second term, the fraction, y, of the Brillouin function, B, is 0.63 or 0.68 %, in excellent agreement with the 0.63 or 0.68 % found in the fit of the temperature dependence of the magnetic susceptibility of **1** or **1**$(H_2O)_9$, see Figure S2 or Figure 5, respectively.

At fields between ca. ±2 T the magnetisation results from the Fe(III) impurity present. But at ca. ±2 T the magnetisation of this impurity is saturated and no longer increases with the applied field. As a consequence, the 2 K magnetisation between ±2 and ±6 T is dominated by the core diamagnetism of **1** or **1**$(H_2O)_9$ and the small diamagnetic contribution of the sample holder and, hence, the observed magnetisation decreases linearly between 2 and 6 T and increases between -2 and -6 T, as shown in Figures 6 and S4. The very small 2 K magnetisation and its field dependence again support the presence of strong antiferromagnetic coupling in the dinuclear units present in **1**.

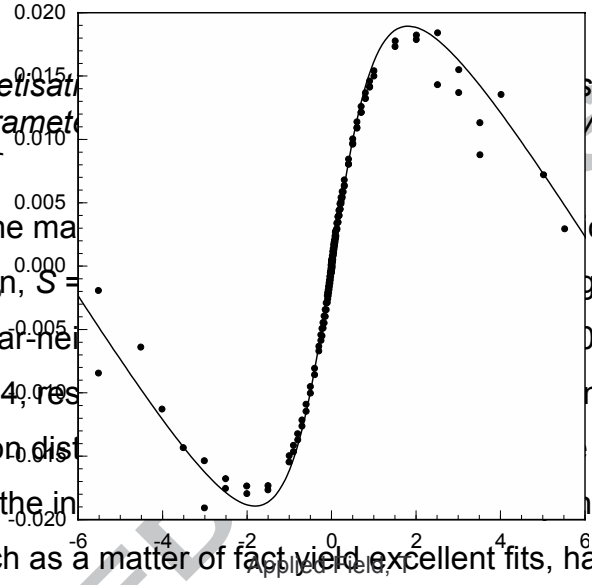

*Figure 6. The 2 K magnetisati[illegible]s a simulation with equation (4) and the paramet[illegible]ve for **1** is shown in Figure S4.*

The above analysis of the ma[illegible]on assumes that all Fe(III) ions are in their high-spin, *S* = [illegible]ghly likely in view of the average Fe(III) to six near-nei[illegible]071(2), 2.076(2), 2.085(2), and 2.083(2) Å, for Fe1-4, res[illegible]nds. However, in spite of these similar coordination dist[illegible] that all or some of the Fe(III) ions are in either the in[illegible]e low, *S* = 1/2, spin state. These possibilities, which as a matter of fact yield excellent fits, have been investigated and the results are discussed in detail in the supplementary information (Table S3, Figure S5).

3.4. Structure & Magnetic Discussion

Among several hundred dinuclear Fe-O-Fe units found in the CDCD database,[18] there are only ten structurally characterised dinuclear species with the FeN_5O environment observed in compound **1** and only two of these have been magnetically characterised, see the top two lines in Table 4 In these two cases[11, 12] the antiferromagnetic exchange coupling constants, –180 and –208 cm^{-1}, are less negative than both values found for the three dinuclear ions in compound **1**. However, the *J* value of –220 cm^{-1} assigned to Fe33a and Fe44b is in reasonable agreement with the value of –208 cm^{-1} found in FIQREC. This agreement is not unexpected because the Fe-O bond distances and the Fe-O-Fe bond angles are very similar in these compounds, see Table 4. The slightly shorter Fe-O bond distances in **1** lead to a more negative *J* value.

Table 4. Magnetic and structural parameters of all the structurally and magnetically characterised dinuclear N_5Fe-O-FeN_5 and Fe-O-Fe ions with additional $(SO_4)^{2-}$ bridges reported to date.

CCDC code	Bridge	Fe-O-Fe (º)	Fe-O (Å)	J (cm^{-1})	Reference

FAJQAK	μ-O	171.4	1.788(4) 1.805(4)	–180	[5, 12]	[a]The average value of J for the two Fe33a and Fe44b sites and for the Fe12 site in **1**$(H_2O)_9$.
FIQREC	μ-O	180	1.8034(10)	–208	[11, 12]	
1 (Fe33a)	μ-O	180	1.7903(6)	–220(2)[a]	this work	
1 (Fe44b)	μ-O	180	1.7940(6)	–220(2)[a]	this work	
1 (Fe12)	(μ-O)(μ-SO_4^{2-})	132.7	1.8118(18) 1.7939(17)	–716(32)[a]	this work	
KAVJEW	(μ-O)(μ-SO_4^{2-})$_2$	122.1	1.833(10) 1.815(11)	–196	[33]	

In contrast, the CCDC shows only four structurally characterised Fe-O-Fe dinuclear species also having an additional SO_4^{2-} bridge [7-10], as observed in dication Fe12 in compound **1** (see Table 5). Unfortunately, none of these dinuclear species has been magnetically characterised and, therefore, our study is the first magnetic characterisation of such a Fe-O-Fe unit with an additional $(SO_4)^{2-}$ bridge. If we search the CSD for Fe-O-Fe species with two or more additional $(SO_4)^{2-}$ bridges, then we find only one magnetically characterised cluster (CSD code KAVJEW) [33]. In this cluster the reported magnetic coupling (J = –196 cm^{-1}, Table 4) is much less negative than the one observed for Fe12 (J = –716 cm^{-1}) . The stronger coupling observed in Fe12 might be due to the cooperative addition of two factors: (i) a much larger Fe-O-Fe bond angle (132.77º in Fe12 compared to 122.1º in KAVJEW) and (ii) shorter Fe-O_{oxido} bond distances (average 1.803 Å in Fe12 compared to 1.824 Å in KAVJEW, Table 4). Both factors result in a much better orbital overlap in Fe12 and, therefore, in a stronger antiferromagnetic coupling.

Table 5. Structural parameters of all the reported Fe-O-Fe-containing compounds containing an additional sulfato bridge.

CCDC code	Fe-O-Fe (º)	Fe-O_{oxido} (Å)	Fe-$O_{sulfato}$ (Å)	Fe-O-O-Fe (º)[a]	Ref
GODXOO	134.34	1.7915(13) 1.8060(13)	1.9644(16) 2.0219(15)	8.72	[10]
NIFBEK	128.60	1.796(18) 1.815(10)	2.03(2) 1.951(7)	37.44	[9]
PIKYIS	133.03	1.7883(18) 1.807(2)	2.012(5) 1.950(6)	7.68	[8]
ZATFIJ	132.37	1.809(10) 1.802(10)	1.983(10) 1.978(10)	4.21	[7]
1 (Fe12)	132.77	1.8118(18) 1.7939(17)	1.940(6) 2.007(10)	20.95	this work

[a]Torsion angle in the sulfato bridge. **4.**

Concluding Remarks

The results presented and discussed above have shown that $Co_2Fe_4O_2(CN)_{12}(tpa)_4$, **1**, has two quite different dinuclear μ-oxido-iron(III) species, first a Fe12 dication, and second, two Fe33a and Fe44b dianions, each octahedrally-based, and weighted as 1 Fe12, ½ Fe33a, and ½ Fe44b, for a total of two exchange-coupled Fe(III) dinuclear species and thus for the

total of four Fe(III) ions in **1**. The dicationic Fe12 unit has an additional sulfato-bridging pathway, involving Fe1-O-S-O-Fe2 whereas the Fe33a and Fe44b dianionic units have, at each Fe(III) ion, a monodentate coordinating diamagnetic hexacyanidocobaltate(III) ion, using one cyanide bridging with N to the iron(III) ion. No other species than **1** were found when applying variations in the synthesis. Clearly electroneutrality from 1 Fe12 dication and ½ Fe33a plus ½ Fe44b dianions has been reached resulting in a stable crystalline product.

Given the different dinuclear Fe(III) sites, perhaps one might expect that the major intermolecular magnetic exchange coupling should primarily go via the linear Fe-O-Fe bridging oxygen and perhaps less via the oxido-sulfato bridge. However, our fits agree most with two exchange parameters i.e. a J_2 of some –220 cm^{-1} (tentatively assigned to the linear Fe–O–Fe) and a more negative J_1 of about –700 cm^{-1}, tentatively assigned to the dinuclear species with both the oxido and sulfato bridge (Fe12). Fits with other spin states for Fe(III), although chemically unlikely, are presented in the ESI. It should be noted that, based only on the magnetic data, it is impossible to distinguish between a model in which all the iron(III) ions have $S_1 = S_2 = 5/2$ and one in which one-half of the iron(III) ions have $S_1 = S_2 = 5/2$ and one-half have $S_1 = S_2 = 3/2$.

If the negative of the antiferromagnetic exchange coupling parameter, $-J$, and the average Fe-O bond distances for the Fe33a and Fe44b sites are added to the Figure 1 of Gorun et al. [34], they coincide exactly with the exponential fit shown in this figure. As expected, the values for the Fe12 site do not agree at all with the values and exponential fit found in this figure.

Finally, it should be noted that several compounds, that effectively are diamagnetic because they have a Heisenberg $S = 0$ electronic spin ground state, have been reported in the literature. For instance, this is the case for $[(TPC)_2Fe_2(\mu\text{-}O)]\cdot 4CHCl_3$ with $J = -265$ cm^{-1}, where TPC is the 5,10,15,20-tetraphenylporphyrinato ligand [35], and $[(bpy)_2Cl_2Fe_2(\mu\text{-}O)(AcO)_2]\cdot CH_3CN$ with J = –264 cm^{-1}, where bpy is 2,2'-bipyridine and AcO is acetate [36]. Several further examples of μ-oxido-bridged dinuclear Fe(III) compounds that are effectively diamagnetic at temperatures up to ca. 300 K may be found in the extensive table published by Weihe and Güdel [37]. Surprisingly, there is no obvious bond metric that seems to account for the strong antiferromagnetic exchange in these compounds.

Conflicts of interest

There are no conflicts to declare.

Appendix A. Supplementary data.

CCDC 1812913 contains all the supplementary crystallographic data for the title compound. These data can be obtained free of charge via http://www.ccdc.cam.ac.uk/conts/retrieving.html, or from the Cambridge Crystallographic Data Centre, 12 Union Road, Cambridge CB2 1EZ, UK; fax: (+44) 1223-336-033; or e-mail: deposit@ccdc.cam.ac.uk.

Supplementary data associated with this article can be found, in the online version, at http://dx.doi.org/#########.

Table S1 shows the important bonding angles around the metal ions. Table S2 lists the correlation between the parameters in the refinement of the magnetic fits. Table S3 shows exchange parameter assuming that some of the Fe(III) has a spin 1/2 and 3/2. Table S4 list the correlation between the parameters for hypothetical cases where some Fe(III) has spin 1/2 and 3/2.

Figure S1 shows the structure and numbering of the anionic unit Fe44a.
Figure S2 shows the fit of the magnetic susceptibility for **1**, Figure S3 shows the fit of the magnetic susceptibility for **1**$(H_2O)_9$ with one exchange coupling constant for all three dinuclear units. Figure S4 shows the magnetisation of compound **1** at 2 K.
Figure S5 shows some fits for hypothetical cases where some Fe(III) has spin 1/2 and 3/2.
Figure S6. Thermogravimetric analysis and differential scanning calorimetric plot of **1**$(H_2O)_9$ measured under N_2 atmosphere at a scan rate of 10 ºC/min.
Figure S7. Simulated and experimental X-ray powder diffraction patterns for compound **1**$(H_2O)_9$.

Acknowledgements

The authors are in debt to the Algerian DG-RSDT (Direction Générale de la Recherche Scientifique et du Développement Technologique) and Université Ferhat Abbas Sétif 1 for financial support. SZ thanks Dr Ewa Juszyńska-Gałązka, from the Institute of Nuclear Physics Polish Academy of Sciences, for performing FT-IR measurements using EXCALIBUR FTS-3000 spectrometer. The magnetic part was supported by the Generalitat Valenciana (PrometeoII/2014/076 project) and the Spanish MINECO (project CTQ2017-87201-P AEI/FEDER, UE).

References

1. O. Kahn, Struct. Bond. 68 (1987) 89-167.
2. O. Kahn, Chem. Phys. Lett. 265 (1997) 109-114.
3. O. Kahn, Philos. Trans. R. Soc. A-Math. Phys. Eng. Sci. 357 (1999) 3005-3023.
4. O. Kahn, O. Cador, J. Larionova, C. Mathonière, J.P. Sutter, L. Ouahab, Mol. Cryst. Liq. Cryst. Sci. Technol. Sect. A 305 (1997) 1-16.
5. C.J. O'Connor, Prog. Inorg. Chem. 29 (1982) 203-283.
6. L. Que, A.E. True, Prog. Inorganic Chem. 38 (1990) 97-200.
7. N. Arulsamy, P.A. Goodson, D.J. Hodgson, J. Glerup, K. Michelsen, Inorg. Chim. Acta 216 (1994) 21-29.
8. C.M. Smith, R.E. Norman, Acta Cryst. E 63 (2007) m2480-m2481.
9. Y. Peng, S. Yan, D. Liao, Z. Jiang, P. Cheng, Chem. J. Chin. Univ 25 (2004) 221-226.
10. A.R. Parent, T. Nakazono, S. Lin, S.S. Utsunomiya, K. , Dalton Trans. 43 (2014) 12501-12513.
11. G. Roelfes, M. Lubben, K. Chen, R.Y.N. Ho, A. Meetsma, S. Genseberger, R.M. Hermant, R. Hage, S.K. Mandal, Z. Young, V. G., Y. Zang, H. Kooijman, A.L. Spek, L. Que, B.L. Feringa, Inorg. Chem. 38 (1999) 1929-1936.
12. J.W. Shin, S.R. Rowthu, J.E. Lee, H.I. Lee, K.S. Min, Polyhedron 33 (2012) 25-32.
13. P. Gomezromero, E.H. Witten, W.M. Reiff, G. Backes, J. Sandersloehr, G.B. Jameson, J. Am. Chem. Soc. 111 (1989) 9039-9047.
14. P. Gomezromero, E.H. Witten, W.M. Reiff, G.B. Jameson, Inorg. Chem. 29 (1990) 5211-5217.
15. R.E. Norman, R.C. Holz, S. Menage, C.J. Oconnor, J.H. Zhang, L. Que, Inorg. Chem. 29 (1990) 4629-4637.
16. G.L. Parrilha, C. Fernandes, A.J. Bortoluzzi, B. Szpoganicz, M.D. Silva, C.T. Pich, H. Terenzi, A. Horn, Inorg. Chem. Commun. 11 (2008) 643-647.

17. F.H. Allen, Acta Crystallogr. Sect. B-Struct. Sci. 58 (2002) 380-388.
18. CSD, in, The Cambridge Crystallographic Data Centre, UK CSD 2017 update., Cambridge Crystallographic Data Centre, UK, 2017.
19. D. Guo, S.Z. Zhan, C.W. Yuan, Transit. Met. Chem. 25 (2000) 299-301.
20. S. Tanase, J. Reedijk, Coord. Chem. Rev. 250 (2006) 2501-2510.
21. M.A. Roman, O.S. Reu, S.I. Klokishner, J. Phys. Chem. A 116 (2012) 9534-9544.
22. A. Mondal, Y.L. Li, M. Seuleiman, M. Julve, L. Toupet, M. Buron-Le Cointe, R. Lescouezec, J. Am. Chem. Soc. 135 (2013) 1653-1656.
23. T. Shiga, T. Tetsuka, K. Sakai, Y. Sekine, M. Nihei, G.N. Newton, H. Oshio, Inorg. Chem. 53 (2014) 5899-5901.
24. M. Roman, S. Decurtins, S.X. Liu, S. Klokishner, Eur. J. Inorg. Chem. (2016) 5324-5331.
25. Bruker, in: Bruker (Ed.), Bruker APEX2, SAINT and SADABS, Bruker AXS Inc., Madison, Wisconsin, USA, 2008, Bruker AXS Inc., APEX2, SAINT and SADABS, Madison, 2008.
26. G.M. Sheldrick, Acta Cryst. (C) 71 (2015) 308.
27. A.L. Spek, Acta Cryst. (C) 71 (2015) 9-18.
28. A.L. Spek, Acta Cryst. D 65 (2009) 148-155.
29. T. Williams, C. Kelley, G. Elber, in, Gnuplot McIntosh, version 3.7, 1999.
30. G.A. Bain, J.F. Berry, J. Chem. Educ. 85 (2008) 532-536.
31. O. Kahn, Molecular Magnetism, Wiley-VCH, New York, 1993.
32. C. Pascanut, N. Dragoe, P. Berthet, J. Magn. Magn. Mater. 305 (2006) 6-11.
33. K. Wieghardt, S. Drueke, P. Chaudhuri, U. Florke, H.J. Haupt, B. Nuber, J. Weiss, Z.Naturforsch.(B) 44 (1989) 1093-1101.
34. S.M. Gorun, S.J. Lippard, Inorg. Chem. 30 (1991) 1625-1630.
35. S.H. Strauss, M.J. Pawlik, J. Skowyra, J.R. Kennedy, O.P. Anderson, K. Startalian, J.L. Dye, Inorg. Chem. 26 (1987) 724-730.
36. J.B. Vincent, J.C. Huffmann, G. Christou, Q. Li, M.A. Nanny, D.H. Hendrickson, R.H. Fong, R.H. Fish, J. Am. Chem. Soc. 110 (1988) 6898-6898.
37. H. Weihe, H.U. Güdel, J. Am. Chem. Soc. 119 (1997) 6539-6544.

TOC-Graphical abstract Polyhedron S-18-00778

Synthesis, structure and magnetic properties of an unusual oligonuclear iron(III)-cobalt(III) compound with oxido-, sulfato- and cyanido-bridging ligands

Fatima Setifi*, Zouaoui Setifi, Piotr Konieczny, Christopher Glidewell, Samia Benmansour, Carlos J. Gómez-García*, Fernande Grandjean, Gary J. Long*, Robert Pelka, Jan Reedijk*

A dinuclear CN-Fe-units

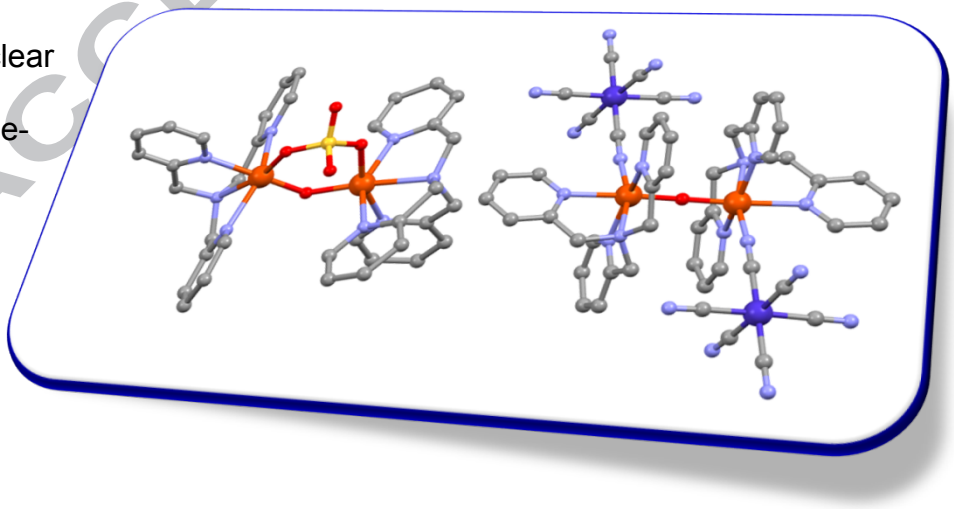

combination of Fe-O-Fe and tetranuclear Co-O-Fe-NC-Co with strong intramolecular antiferromagnetic coupling.

TOC-Graphical abstract Polyhedron S-18-00778

Synthesis, structure and magnetic properties of an unusual oligonuclear iron(III)-cobalt(III) compound with oxido-, sulfato- and cyanido-bridging ligands

Fatima Setifi*, Zouaoui Setifi, Piotr Konieczny, Christopher Glidewell, Samia Benmansour, Carlos J. Gómez-García*, Fernande Grandjean, Gary J. Long*, Robert Pelka, Jan Reedijk*

A combination of dinuclear Fe-O-Fe and tetranuclear Co-CN-Fe-O-Fe-NC-Co units with strong intramolecular antiferromagnetic coupling.